2006

Modeling the Transient Behavior of an Active Magnetic Regenerative Refrigerator

Kurt Engelbrecht
University of Wisconsin

Gregory Nellis
University of Wisconsin

Sanford Klein
University of Wisconsin

Modeling the Transient Behavior of an Active Magnetic Regenerative Refrigerator

Kurt Engelbrecht*, Greg Nellis, and Sanford Klein

University of Wisconsin, Mechanical Engineering,
Madison, WI, USA
(608 263-2613, Fax 608 262 8464, kengelbrecht@wisc.edu)

ABSTRACT

Active magnetic regenerative refrigeration (AMRR) systems represent an environmentally attractive space cooling alternative because they do not require a synthetic working fluid. Previous work has shown that AMRR systems have the potential to be as efficient as vapor compression systems provided the size of the regenerator is adequately large. However, the transient and part-load characteristics of AMRR systems have not been studied. A numerical AMRR model has been developed that solves the coupled fluid and solid energy balances. The predicted temperature profiles are used to calculate refrigeration capacity, heat rejection, and other cycle parameters. This model is used to predict the startup characteristics and part-load performance of a well-designed AMRR system.

1. INTRODUCTION

Magnetic refrigeration systems use magnetocaloric materials as the working material in a refrigeration cycle. The thermal and magnetic properties of magnetocaloric materials are highly coupled over a specific temperature range, allowing them to be used within energy conversion systems. Temperature (T) and entropy (S) together define the transfer of heat while applied field ($\mu_o H$) and magnetic moment (VM) describe the transfer of magnetic work (Guggenheim, 1967). The fundamental property relation for a magnetocaloric substance is

$$dU = T\,dS + \mu_o\,H\,d\left(V\,M\right) \tag{1}$$

where U is the internal energy. Examination of Eq. (1) reveals that the applied field is analogous to pressure and magnetic moment is analogous to (the inverse of) volume for compressible substances. A more thorough discussion on magnetic refrigeration is given by Yu et al. (2003).

Magnetic cooling has been used in "one-shot" cycle configurations since the 1930s to achieve very low temperatures (Giaque and MacDougall, 1933); these cycles require complex heat switches can provide refrigeration only over a limited temperature lift. These technical barriers have been overcome by the active magnetic regenerative refrigeration (AMRR) cycle where a porous bed of magnetic material is exposed to a time-varying magnetic field and a time-varying flow of heat transfer fluid. Researchers at Astronautics Corporation have demonstrated an AMRR system in which multiple regenerators rotate through the gap of a permanent magnet (Zimm et al., 2002); this system (Fig. 1) represents a practical implementation of the AMRR cycle near room temperature.

Technical advances in cycle configuration and material science (e.g., Chen et al., 2003) have pushed magnetic cooling technology to the point where it is now being seriously considered for several applications. A well-designed magnetic system may be competitive with or even more efficient than vapor compression systems (Engelbrecht, 2005) and the metallic refrigerant has essentially zero vapor pressure and therefore is ecologically sound with no Ozone Depletion Potential (ODP) and zero direct Global Warming Potential (GWP). The AMRR system may also have advantages relative to noise, control, and part load efficiency.

The control of an AMRR system has not been studied previously. However, AMRR systems are inherently variable capacity in that the cooling load can be controlled with the flow rate of heat transfer fluid (i.e., by controlling the pump) or the cycle frequency (i.e., by controlling the motor). This paper briefly discusses a physics-based, numerical model of an AMRR cycle that is subsequently used to investigate the part-load performance of an AMRR-based air-conditioning system obtained by modulating the mass flow rate and frequency. Based on this analysis, the optimal control scheme is identified in terms of the combination of mass flow rate and cycle frequency

that results in the maximum efficiency for a desired cooling rate. A transient analysis of a practical AMR air-conditioning system is also presented which provides some insight into the startup and response time associated with this system.

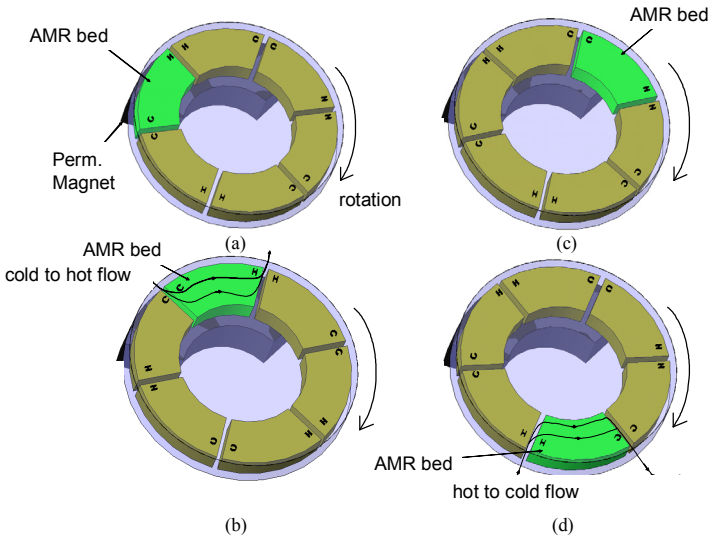

Figure 1: Conceptual drawing showing the processes that make up the rotary AMRR system: (a) magnetization, (b) cold-to-hot flow, (c) demagnetization, and (d) hot-to-cold flow.

2. NUMERICAL MODEL

An AMRR numerical model has been developed that is flexible with respect to operating conditions, geometry, and material and fluid properties. The equipment external to the regenerator bed (e.g., the pumps, drive motor, etc.) are not explicitly modeled; their effect on the bed is felt through an imposed time variation of the mass flow rate and magnetic field ($\dot{m}(t)$ and $\mu_o H(x,t)$) A positive mass flow is entering the hot end of the regenerator bed while a negative flow is entering the cold end of the bed; the flow enters with the temperature of the adjacent reservoir (T_H and T_C). The fluid density (ρ_f) at any location is assumed to be constant so that the mass storage terms in the governing equations are neglected. The remaining required fluid properties, specific heat capacity (c_f), viscosity (μ_f), and thermal conductivity (k_f), are assumed to be functions of temperature but not pressure which is appropriate for a liquid heat transfer fluid. The density of the magnetic material (ρ_r) is assumed to be constant at any location. The partial derivative of entropy with respect to applied field at constant temperature, specific heat capacity, and thermal conductivity of the regenerator matrix are assumed to be functions of temperature and applied field ($\partial s_r / \partial \mu_o H_T (T, \mu_o H)$, $c_r(T,\ \mu_o H)$, and $k_r(T,\ \mu_o H)$). The matrix configuration is characterized by a hydraulic diameter (d_h), porosity (ε), and specific surface area (a_s). The Nusselt number of the matrix is assumed to be a function of the local Reynolds number and Prandtl number of the fluid ($Nu(Re_f,\ Pr_f)$). The friction factor is assumed to be a function of the local Reynolds number ($f(Re_f)$). The matrix/fluid composite is characterized by an effective thermal conductivity (k_{eff}) and the overall size of the regenerator is specified according to its length (L) and total cross-sectional area (A_c).

The fluid and regenerator temperature variations over a periodic steady-state cycle are the output of this model ($T_f(x,t)$ and $T_r(x,t)$) and can, when coupled with the prescribed mass flow rate and applied field, be used to calculate various cycle performance metrics such as refrigeration load and input power associated with the magnetic field. The temperature history is governed by a set of coupled, partial differential equations in time and space that are derived from energy balances on the fluid and matrix. After some simplification, the energy balance on the fluid is:

$$\dot{m}\, c_f \frac{\partial T_f}{\partial x} + \frac{Nu\, k_f}{d_h} a_s\ A_c \left(T_f - T_r\right) + \rho_f\ A_c\ \varepsilon\ c_f \frac{\partial T_f}{\partial t} - k_{disp} A_c \frac{\partial^2 T_f}{\partial x^2} = \left| \frac{f_f\, \dot{m}^3}{2\, \rho_f^2\, A_c^2\, d_h} \right| \qquad (1)$$

where the terms represent (in order from left to right) the enthalpy change of the flow, heat transfer from the fluid to the magnetic material, energy storage, energy transfer due to axial dispersion associated with mixing in the fluid, and viscous dissipation. The governing equation for the matrix is:

$$\frac{Nu\, k_f\, a_s}{d_h}\left(T_f - T_r\right) + k_{eff}\frac{\partial^2 T_r}{\partial x^2} = \left(1-\varepsilon\right)\rho_r\, T_r \frac{\partial s_r}{\partial \mu_o H}_T \frac{\partial \mu_o H}{\partial t} + \left(1-\varepsilon\right)\rho_r\, c_{\mu_o H}\frac{\partial T_r}{\partial t} \tag{2}$$

where the terms represent heat transfer from the fluid to the regenerator, non-dispersive or static axial conduction (through the composite of the regenerator and fluid), magnetic work transfer, and energy storage.

The numerical solutions for the fluid and regenerator temperatures are obtained on a numerical grid that extends from 0 to L in space and from 0 to τ in time. These equations are linearized and discretized and the resulting set of algebraic equations is solved; the numerical method takes spatially implicit but temporally explicit steps in time until the end of the cycle. The results of the calculation are the fluid and regenerator temperatures at all spatial nodes and for each time step over an entire cycle. Therefore, the model is capable of predicting either the transient or the cyclic steady state operation of an AMRR bed. To determine when a cyclic steady state has been reached, the change in the total energy of the regenerator and the fluid between the beginning and end of each cycle is evaluated and this quantity is compared to the maximum change in the total energy of the bed and fluid during the cycle. When this dimensionless value of the absolute change in energy of the regenerator from cycle to cycle is less than 0.02% then steady state has been achieved. This model has been implemented in MATLAB and is an extension of the fully implicit model presented in Engelbrecht (2005).

The assumption underlying the one-dimensional regenerator model is that the true temperature distribution within the regenerator material at any position can be adequately represented by a single temperature at any time. However, the Biot number associated with a magnetic material (which may have a low conductivity) interacting with a liquid heat transfer fluid (which will provide a relatively high heat transfer coefficient) is not generally small throughout the cycle; therefore, the temperature gradients within the regenerator matrix may not be negligible. This effect has been studied in detail using a local model of a single sphere within experiencing a sinusoidal variation of the applied field while communicating with a fluid at constant temperature (Engelbrecht et al., 2006). The impact of the internal temperature gradients in the sphere (which prevent all of the material in the sphere from participating in the cycle) can be approximately accounted for by modifying the heat transfer coefficient based on the Biot number and Fourier number; a technique that has been suggested by Jeffreson (1972) in the context of a passive regenerator. It is important to correctly account for the effect of internal temperature gradients in the AMRR material, particularly for parametric studies that consider a large range of operating frequencies.

3. TRANSIENT OPERATION

In order to model the transient operation of an AMRR system, the regenerator model discussed in the previous section is coupled with simple models of the hot and cold heat exchangers. The AMRR system uses a liquid heat transfer fluid and therefore the heat capacity of the fluid in the pipes connecting the regenerator and heat exchanger is significant relative to the heat capacity of the heat exchangers and the bed, and it must be considered. For this analysis, the total heat capacity of the heat exchangers, heat transfer fluid, and tubing are broken into three parts corresponding to the upstream reservoir (the pipe and fluid upstream of the heat exchanger), the heat exchanger itself and the associated entrained fluid, and the downstream reservoir (the pipe and fluid downstream of the heat exchanger); this model is adopted for both the hot and cold heat exchanger circuits so that a total of six thermal masses (exclusive of the bed itself) are considered.

In order to determine the size of each thermal mass, the size of the heat exchangers and the length of pipe connecting them to the active regenerator bed were specified. These pipes were sized by running the DOE/ORNL Heat Pump Design Model developed by Rice (2005) using its default inputs, which correspond to a domestic air conditioning system with a capacity of 2.5 ton. The use of the DOE/ORNL model ensures that the AMRR system that is considered has external hardware that is nominally equivalent to a comparably sized vapor compression system. A unique design aspect of an AMRR system is that there is no phase change associated with the passage of the heat transfer fluid through either the hot or cold heat exchangers (which are analogous to the condenser and

evaporator) and the temperature rise/fall of the heat transfer fluid in these heat exchangers is less than 5 K in any practical system. As a result, the fluid mass flow rate in the AMRR system must be substantially larger than in a vapor compression cycle with comparable capacity. The approximate ratio of mass flow rates for an AMRR system ($\dot{m}_{AMRR}$) to the mass flow rate for a vapor compression system ($\dot{m}_{vc}$) is given by:

$$\frac{\dot{m}_{AMRR}}{\dot{m}_{vc}} \sim \frac{\Delta h_{v,ref}}{c_f \Delta T_{mc}} \tag{3}$$

A typical value of the temperature rise due to the magnetocaloric effect, ΔT_{mc}, is 2 K when water is used as the heat transfer fluid; Eq. (2) suggests that the required AMRR mass flow rate will be approximately 20 times the mass flow rate of R22 required by an equivalent vapor compression system. To avoid large pumping losses due to the increased fluid flow, the diameter of the connecting tube is increased from 6.4 mm (the DOE/ORNL model value) to 37 mm for this analysis. Otherwise, the outputs from the DOE/ORNL model were used to determine the total heat capacity of the heat exchangers and connecting tubing. The total length of tubing is 14.6 m to the cold heat exchanger and 0.6 m to the hot heat exchanger (consistent with an air-conditioning system that is placed out-of-doors near the hot heat exchanger). The increased tube size and high heat capacity of water make the total heat capacity of the upstream and downstream reservoirs associated with the cold heat exchanger circuit quite large. The heat capacities of the reservoirs that are modeled in this analysis are summarized in Table 1; all values in Table 1 include the heat capacity of the fluid, tubing, and fins, if applicable.

Table 1: Calculated system heat capacities

Component	Hot Side Heat Capacity	Cold Side Heat Capacity
upstream reservoir	30200 J/K	724300 J/K
heat exchanger	15300 J/K	11200 J/K
downstream reservoir	30200 J/K	724300 J/K

The numerical model was used to predict the transient performance of an AMR system for several conditions. In order to simulate transient operation, the regenerator is started from a specified initial temperature distribution and the model is stepped forward in time for one cycle to reach a new regenerator temperature distribution. The temperature of the fluid entering the regenerator from the hot and cold downstream reservoirs is assumed constant during the cycle. The temperature of fluid exiting the regenerator is assumed to mix perfectly in the upstream reservoir and therefore enters the heat exchanger at a uniform temperature. The hot heat exchanger is modeled as a cross-flow, air-to-liquid heat exchanger using an *ε-NTU* method. Analysis of the cold heat exchanger considers the condensation that takes place; heat transfer and moisture removal for the cold heat exchanger are modeled using a heat transfer analogy that is similar to the *ε-NTU* method presented by Braun et al. (1989). The heat transfer accepted or rejected by the heat exchanger is determined and the fluid exiting the heat exchanger is assumed to mix perfectly in the downstream reservoir and the new temperature provided to the AMRR for the following cycle is calculated with an energy balance. The system parameters used in this study are given in Table 2 and correspond to an optimally designed AMRR system for domestic air conditioning, as discussed in Engelbrecht et al. (2006).

Table 2: System parameters used for transient study

Parameter	Value	Parameter	Value
maximum applied field	1.5 Tesla	heat transfer fluid	Water
cold air flow rate	0.57 kg/s	fluid mass flow rate	1.4 kg/s
hot air flow rate	1.42 kg/s	Period	0.2 sec (5 Hz)
cold heat exchanger UA	880 W/K	sphere size for packing	0.2 mm
hot heat exchanger UA	1430 W/K	motor efficiency	0.9
regenerator volume	10 L	pump efficiency	0.7
regenerator type	packed sphere	cycle time (τ)	0.5 s

The startup response of an AMRR system that is entirely at a uniform temperature of 300 K (~80ºF) was simulated and the response, presented in terms of refrigeration capacity as a function of time, is shown in Figure 2a. Note that

the temperature of the air entering the hot and cold heat exchangers is assumed to be constant and equal to 300 K.

Another transient condition of interest corresponds to a system that has reached steady state and is then shut off for a short period and restarted. This corresponds to modulation of the capacity through on/off control; the subsequent section shows that there are more efficient control strategies for an AMRR system; however, the transient response under these conditions is still of interest. Kim and Bullard (2001) measured the dynamic response of a vapor compression air-conditioning system using R-410A under this type of transient operation; in order to compare the transient performance of an AMRR system directly to a vapor compression system, the test conditions reported by Kim and Bullard were used to simulate the transient performance of an AMRR system. The regenerator and hot heat exchanger circuit are assumed to start from a uniform temperature of 308 K (corresponding to being placed in a warm, outdoor environment) while the cold circuit starts at a uniform temperature of 300 K (corresponding to its placement in a previously conditioned, indoor environment). The temperature of the air entering the heat exchangers is assumed to be constant and equal to the temperature of either the surroundings or cooled space. The temperatures of the upstream reservoirs, which are the temperatures of the fluid that enters the regenerator during each cycle, are shown in Figure 2b as a function of time.

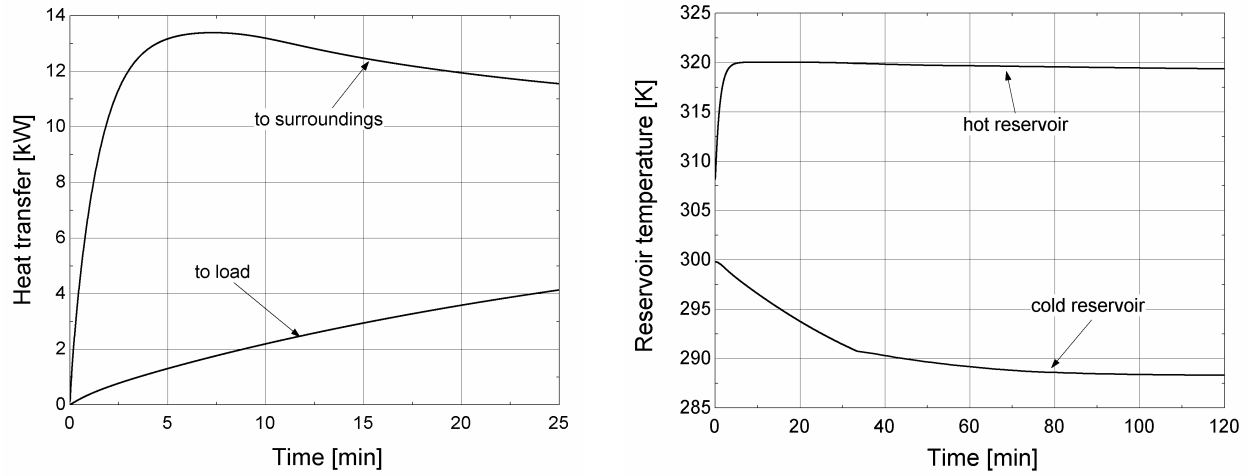

Figure 2: Transient operation of an AMRR; (a) refrigeration capacity of a system started from a uniform temperature of 300 K, (b) reservoir temperature as a function of time for the system that is shut off and restarted

Figure 2a shows that the heat transfer in the hot heat exchanger increases much more rapidly than the heat transfer in the cold heat exchanger, and Figure 2b shows that the hot reservoir temperature also exhibits a much faster response than the cold circuit because the tubing to the cold heat exchanger is much longer than to the hot heat exchanger and therefore the cold circuit heat capacity is much higher. Kim and Bullard reported that the vapor compression system took approximately 15 min to reach steady state after it was restarted and Figure 2b shows that the AMRR system took approximately 120 min under the same conditions. However, the relatively fast response of the hot reservoir shows that if the length of the connecting tubing to the cold heat exchanger were reduced, the transient response time of the AMRR system would also be significantly reduced.

4. PART LOAD PERFORMANCE

AMRR systems are variable coolers as the cooling capacity may be controlled by varying the flow rate the heat transfer fluid, the cycle time, or both. To investigate the dependence of efficiency on cycle time and mass flow rate, the performance of a single system was predicted over a range of fluid mass flow rates and cycle times (corresponding to varying the pump and motor speeds). The system parameters are summarized in Table 3; note that the AMRR model alone was used to predict the performance and the heat exchangers were not considered. The dwell ratio listed in Table 3 is the portion of the cycle time when there is no fluid flow and the aspect ratio is the ratio of the regenerator length to diameter. The results of the parametric study are presented in terms of the coefficient of performance as a function of cooling power provided by the system for constant values of the heat transfer fluid mass flow rate, $\dot{m}$, and cycle time, τ. The refrigeration capacity and coefficient of performance are complicated functions of cycle time and mass flow rate, and the results are summarized in Figure 3.

Table 3: Parameters used for space cooling part load performance.

Parameter	Value	Parameter	Value
heat rejection temp.	287 K	sphere size for packing	0.2 mm
load temperature	310 K	number of beds	6
dwell ratio	0.5	pump efficiency	0.7
maximum applied field	1.5 Tesla	motor efficiency	0.9
total regenerator volume	8 L	heat transfer fluid	Water
regenerator aspect ratio	0.25	regenerator type	packed sphere

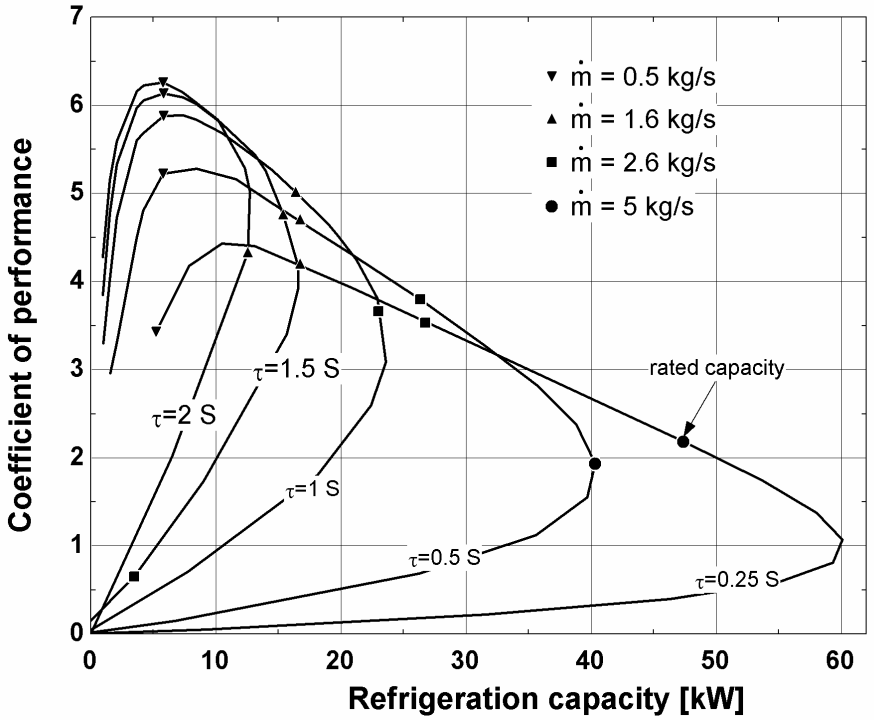

Figure 3: *COP* as a function of cooling power for various values of cycle time and fluid mass flow rate

Figure 3 can be used to determine the optimum cycle time and mass flow rate for a given refrigeration capacity. The best operating condition is the curve that results in the highest *COP* for the desired cooling capacity. Studying curves of constant cycle time reveals that the system is capable of producing the same cooling power with two unique coefficients of performance. The lower *COP* corresponds to operation at a fluid flow rate that is too large for the regenerator. At high cycle times (i.e., low frequency), the number of times the material is magnetized and demagnetized per unit time decreases and therefore maximum attainable cooling power decreases; for example, at τ=0.5 s, the maximum cooling power is approximately 40 kW whereas τ=2 s would provide at most 13 kW. However, at low cycle times (i.e., high frequency) there is not sufficient time for heat transfer and therefore *COP* decreases.

Lines of constant mass flow rate are harder to study in Figure 3 because some mass flow rates are not at all appropriate for certain frequencies and therefore these operating conditions do not appear on the figure. However, the cooling capacity initially increases with increasing flow rate but the regenerator eventually becomes overwhelmed and the cooling capacity begins to decrease and can become negative; this trend is especially evident by examining those points that correspond to $\dot{m}$=2.6 kg/s where the refrigeration capacity is approximately equal for cycle time of 0.25 – 1 s but then decreases dramatically for a cycle time of 1.5 s.

The optimum fluid flow rate and cycle time combinations correspond to traversing the apex of the curves shown in Figure 3 and provide the highest COP at a given capacity. These points were estimated for several refrigeration capacities and the results are shown in Figure 4a. The optimal modulation strategy requires simultaneous control of the pump and the motor; a simpler control strategy would vary only one of these control parameters. The *COP* and refrigeration capacity were calculated when the cycle time was held constant and the fluid mass flow rate varied (pump modulation) and also when the fluid flow was held constant while the cycle time varied (frequency modulation) and the results are shown in Figure 4b. Notice that when the desired refrigeration capacity is near the design point, modulation of only the fluid mass flow rate (or pump speed) is effective and yields efficiencies that are very near the optimum control scheme. However, as the desired cooling rate becomes relatively small, it becomes beneficial to vary the cycle time as well. When only the cycle time is modulated, the bed quickly becomes overwhelmed by the fluid flow and the efficiency decreases quickly; clearly for the design considered here modulating the fluid flow rate is more attractive than modulating the cycle time, especially near the design point.

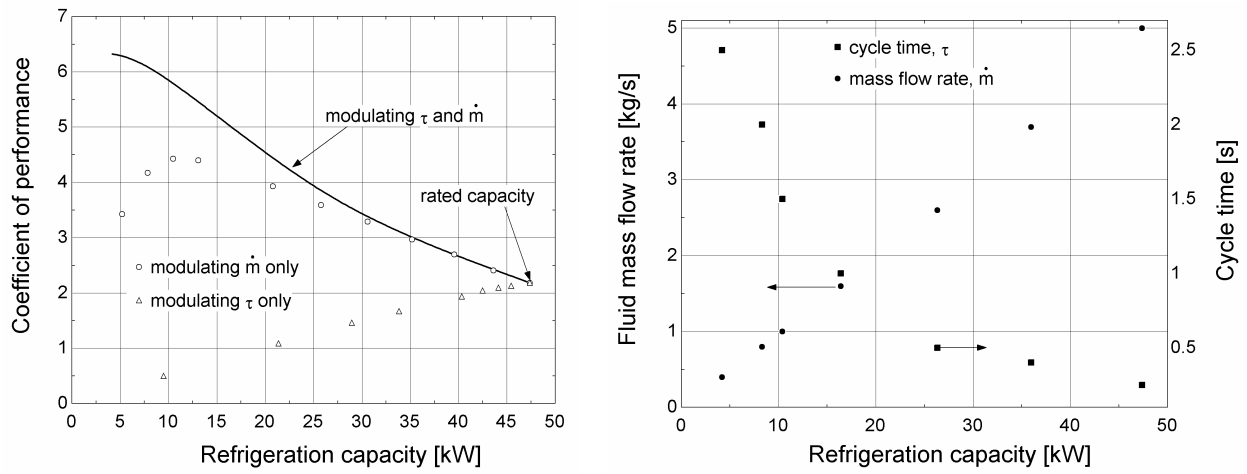

Figure 4: (a)Optimum fluid flow rate and cycle time as a function of refrigeration capacity and (b) comparison of modulating only fluid mass flow rate or cycle time to control desired cooling capacity

5. CONCLUSIONS

This paper studied the transient and part load operation of a well-designed AMRR system used for residential air-conditioning. The analysis shows that part load operation is achieved most efficiently by modulating both the cycle time and the fluid flow rate in order to achieve the desired cooling capacity. Modulating only the fluid flow rate is an effective means of controlling the cooling capacity near the rated capacity, but modulating only the cycle time is never an effective means of controlling the system. The transient response of an AMRR system was found to be significantly slower than a comparable vapor compression system; this is mostly to the high heat capacity of the liquid heat transfer fluid in the connecting tubing which must be very large. The transient response could be improved by reducing the length of the tubing that connects the cold heat exchanger to the regenerator. Note that AMRRs are variable coolers and therefore the cooling capacity of the system could be controlled to match the demanded load which decreases the importance of the transient response of the system.

NOMENCLATURE

A_c	cross-sectional area	(m^2)	T	temperature	(K)
a_s	specific surface area	(1/m)	t	time	(s)
Bi	Biot number ($h\ R/k_r$)	(-)	x	position	(m)
c	specific heat	(J/kg-K)	ΔT_{mc}	adiabatic ΔT with magnetization	(K)
d_h	hydraulic diameter	(m)	$\Delta h_{v,ref}$	enthalpy of vaporization	(J/kg)
f	friction factor	(-)	ε	porosity	(-)
Fo	Fourier number ($k_r \tau / \rho_r\ c_r\ R^2$)	(-)	μ	viscosity	(kg/m-s)
h	heat transfer coefficient	(W/m^2-K)	$\mu_o H$	magnetic field	(Tesla)
h^*	corrected heat trans. coefficient	(W/m^2-K)	ρ	density	(kg/m^3)

k	conductivity	(W/m-K)	τ	cycle time	(s)
L	length	(m)	**Subscripts**		
$\dot{m}$	mass flow rate	(kg/s)	*disp*	dispersion	
Nu	Nusselt number ($h\, d_h / k_f$)	(-)	*eff*	effective	
Pr	Prandtl number	(-)	*f*	fluid	
Re	Reynolds number $\left(\dot{m}\, d_h / A_c \mu\right)$	(-)	*r*	regenerator	
U	internal energy	(J/kg)	*vc*	vapor comp	
S	entropy	(J/kg-K)			

REFERENCES

Braun, J. E., Klein, S. A., Mitchell, J. W., 1989, Effectiveness Models for Cooling Towers, ASHRAE Transactions, vol. 95 part 2: p164-174.

Chen Y., Wang F., Shen B., Hu F., Sun J., Wang G., Cheng Z., 2003, Magnetic properties and magnetic entropy change of $LaFe_{11.5}Si_{1.5}H_y$, J. Phys.: Condens. Matter, vol. 15 no. 7: p. L161.

Engelbrecht, K. L., 2005, A Numerical Model of an Active Magnetic Regenerator Refrigeration System, M.S. Thesis, Mechanical Engineering, University of Wisconsin – Madison.

Engelbrecht, K. L., Nellis, G. F., Klein, S. A., 2006, The Effect of Internal Temperature Gradients on Regenerator Matrix Performance, accepted for publication by Journal of Heat Transfer, Feb. 2006.

Engelbrecht, K. L., Nellis, G. F., Klein, S. A., 2006, Predicting the Performance of an Active Magnetic Regenerator Refrigerator used for Space Cooling and Refrigeration, accepted for publication by HVAC&R Journal.

Giauque, W. F., MacDougall D. P., 1933, Attainment of temperatures below 1º absolute by demagnetization of $Gd_2(SO_4)_3\ 8H_2O$, Phys. Rev, vol. 43: p. 7768.

Jeffreson, C. P., 1972, Prediction of Breakthrough Curves in Packed Beds: I. Applicability of Single Parameter Models, AIChE Journal, vol. 18: p. 409-416.

Kim, H., Didion, C. W., 2001, Dynamic Characteristics of a R-410A Split Air-Conditioning System, Int. J. Refrig., vol. 24: p. 652-659.

K. Rice, 2005, DOE/ORNL Heat Pump Design Model, Mark V & VI Version, http://www.ornl.gov/~wlj/hpdm/

Yu, B. F., Gao, Q., Zhang, B., Meng, X. Z., Chen, Z., 2003, Review on Research of Room Temperature Magnetic Refrigeration, Int. J. Refrig., vol. 26: p. 622-636.

Zimm, C. B., Sternberg, A., Jastrab, A. G., Boeder, A. M., Lawton, Jr. L. M., Chell, J. J., 2002, Rotating Bed Magnetic Refrigeration Apparatus, U.S. Patent Application, US 2002/0053209 A1.

ACKNOWLEDGEMENT

The financial support of Astronautics Corporation and the American Society of Heating and Air-Conditioning Engineers (ASHRAE) is greatly appreciated.